GPS Solut (2017) 21:1583–1591
DOI 10.1007/s10291-017-0635-4

ORIGINAL ARTICLE

Global ionosphere map constructed by using total electron content from ground-based GNSS receiver and FORMOSAT-3/COSMIC GPS occultation experiment

Yang-Yi Sun[1] · Jann-Yenq Liu[1] · Ho-Fang Tsai[2] · Andrzej Krankowski[3]

Received: 7 July 2016 / Accepted: 29 April 2017 / Published online: 13 May 2017

Abstract Effects of rapidly changing ionospheric weather are critical in high accuracy positioning, navigation, and communication applications. A system used to construct the global total electron content (TEC) distribution for monitoring the ionospheric weather in near-real time is needed in the modern society. Here we build the TEC map named Taiwan Ionosphere Group for Education and Research (TIGER) Global Ionospheric Map (GIM) from observations of ground-based GNSS receivers and space-based FORMOSAT-3/COSMIC (F3/C) GPS radio occultation observations using the spherical harmonic expansion and Kalman filter update formula. The TIGER GIM (TGIM) will be published in near-real time of 4-h delay with a spatial resolution of 2.5° in latitude and 5° in longitude and a high temporal resolution of every 5 min. The F3/C TEC results in an improvement on the GIM of about 15.5%, especially over the ocean areas. The TGIM highly correlates with the GIMs published by other international organizations. Therefore, the routinely published TGIM in near-real time is not only for communication, positioning, and navigation applications but also for monitoring and scientific study of ionospheric weathers, such as magnetic storms and seismo-ionospheric anomalies.

✉ Jann-Yenq Liu
jyliu@jupiter.ss.ncu.edu.tw

[1] Graduate Institute of Space Science, National Central University, Taoyuan, Taiwan

[2] Department of Earth Sciences, National Cheng Kung University, Tainan, Taiwan

[3] Space Radio-Diagnostics Research Centre, University of Warmia and Mazury in Olsztyn, Olsztyn, Poland

Keywords Global Ionospheric Map · Total electron content · FORMOSAT-3/COSMIC · Ionospheric weather · GNSS

Introduction

The earth's ionosphere becomes more relevant to human society, as it influences the accuracy of positioning and navigation and the quality of telecommunication (Davies 1990). Based on measurements of ground-based Global Navigation Satellite System (GNSS) networks, the global ionosphere map (GIM) of the total electron content (TEC) is published daily by the International GNSS Service (IGS), the Center for Orbit Determination in Europe (CODE), the European Space Operations Centre (ESOC), the University of Warmia and Mazury (UWM), the NASA's Jet Propulsion Laboratory (JPL), and the Technical University of Catalonia (UPC) (ftp://cddis.gsfc.nasa.gov/gps/products/ionex/) since 1998 (Hernández-Pajares et al. 2009).

Vertical TEC observations from hundreds of ground-based receivers are estimated approximating the ionosphere as a thin layer and are interpolated globally using spherical harmonic expansion (Schaer et al. 1995, 1996, 1998). Scientists have been using the GIM TEC to study ionospheric weather, including the influence of geomagnetic storms on the ionospheric TEC and seismo-ionospheric precursors for recent devastating large earthquakes. Huang et al. (2010) analyzed the GIM TEC and showed the positive phase of the ionospheric storm at the magnetic equator close to sunset near equinox. Jin et al. (2017) studied the positive and negative ionospheric response to the March 2015 strong geomagnetic storm using the GIM TEC map. Liu et al. (2009, 2010, 2011)

reported the temporal and spatial precursors in the GIM TEC of the May 12, 2008, Mw7.9 Wenchuan earthquake, December 26, 2004, M9.3 Sumatra–Andaman Earthquake, and January 12, 2010, Mw7 Haiti earthquake.

However, the TEC from the ground-based receivers is provided mainly over continental regions, which result in the GIM TEC with better accuracy over the land but less accuracy over the ocean. If the GIMs are available in real time, then immediate correction of the positioning and navigation is possible as well as the practical application of monitoring the ionospheric weather.

Radio occultation (RO) observations from FORMOSAT-3/COSMIC (F3/C) provide global TEC observations as well. However, the massive RO dataset has not yet been standardly merged into GIM systems. Therefore, in this study, the Taiwan Ionospheric Group for Education and Research (TIGER) is constructing a GIM by adding F3/C RO data into ground-based GPS and GLONASS TEC (GNSS TEC hereafter) measurements from Taiwan Analysis Center for COSMIC (TACC). The goal of the TIGER GIM (TGIM) is to be published in near-real time with a 4-h time delay having a standard spatial resolution of 2.5° in latitude and 5° in longitude and a high temporal resolution of every 5 min (288 maps per day) for studying the ionospheric weather and for building an ionospheric data assimilation system.

Observation

Both ground-based GNSS TEC and space-based GPS TEC are used in this study. TEC measurements from 123 ground-based GNSS receivers (Fig. 1) provided by TACC are used to construct the TGIM. The GPS consists of more than 24 satellites distributed over six orbital planes and encircling the globe at near 20,200 km altitude. Each GPS satellite transmits radio signals in two L-band frequencies ($f_1 = 1575.42$ MHz and $f_2 = 1227.60$ MHz). Since the ionosphere is a dispersive medium, electron density information can be retrieved from carrier phases and code pseudorange observations obtained from dual-frequency receivers. The slant TEC (STEC), which is the integration of electron density along the ray path from a ground-based GPS receiver (Rx) to a GPS satellite (Tx), can be expressed as

$$\mathrm{STEC} = \int_{Tx}^{Rx} N ds = \frac{1}{40.3}\left(\frac{f_1^2 f_2^2}{f_1^2 - f_2^2}\right)(p_2 - p_1 + \mathrm{res}) \qquad (1)$$

where N is the electron density and s denotes the integration path along a given ray path; p_1 and p_2 are the pseudoranges in meters for the two frequencies, and res is the residual term. The STEC derived from carrier phases can also be levelled based on the pseudorange TEC to increase the accuracy and precision of the measurements significantly. The residual includes satellite differential code biases (DCB) and receiver DCB. Both the DCB values are calibrated with the DCB data provided by CODE. The receiver DCB values are estimated by the least squares method every 2 h (Jin et al. 2012) if the DCB data for receivers are unavailable at CODE. The STEC along the ray path can be converted to the vertical component of VTEC at its associated longitude and latitude (Tsai and Liu 1999), assuming that the greatest electron density in the ionosphere usually is situated near 450 km altitude. GLONASS TEC is derived in the same algorithm as above except for different sounding frequencies.

The ground-based GNSS receivers are widely distributed throughout the world, except for the oceans, deserts, and polar regions. The globally and uniformly distributed measurements recorded by the space-based F3/C RO technique fill the gaps of ground-based observations (Fig. 1). The F3/C mission that consists of six microsatellites with the GPS occultation experiment (GOX) payload carries out atmospheric and ionospheric RO soundings since April 2006. F3/C provides observations of vertical structures of the global ionospheric electron density from 100 km altitude up to the satellite altitude near 800 km. RO observations, particularly from F3/C, have significantly improved our capability of monitoring the global ionosphere. The F3/C RO electron density profiles can be freely downloaded in near-real time (available on the website within 45 min) from the ionPrf file in the second data level, which is processed by the COSMIC Data Analysis and Archive Center (CDAAC, http://cosmic-io.cosmic.ucar.edu/cdaac/index.html) and TACC (http://tacc.cwb.gov.tw/cdaac/index.html), using the Abel inversion technique of TEC along the LEO to GPS path since May 2006.

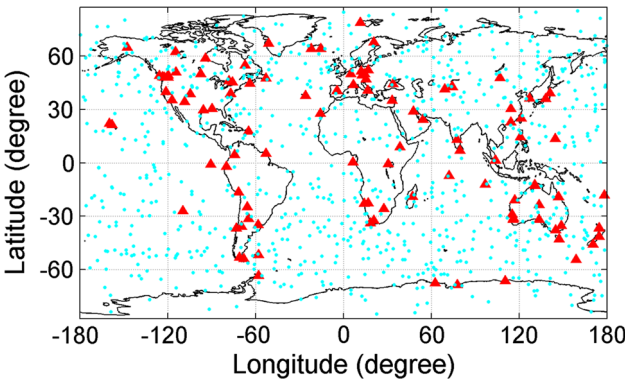

Fig. 1 Global distributions of ground-based GNSS receivers (*red triangles*) from IGS and 1-day F3/C RO soundings (*cyan dots*) reveal that the GNSS receivers are mainly on continents and the F3/C soundings are distributed nearly uniformly around the globe. The *dots* stand for the distribution of daily F3/C observations, and *red triangles* refer to 123 ground-based GPS/GLONASS receivers

The F3/C also provides an opportunity to observe the morphology and variations in the inner magnetosphere in the planetary scale above 800 km altitude. Based on the dual-frequency difference, the F3/C measurement can be converted to differential code biases (DCB)-calibrated, multipath-calibrated plasmaspheric electron content. The plasmaspheric content can reach up to about 12 TECU around the dayside magnetic equator (Zhang and Tang 2014). The F3/C TEC we used is the sum of F3/C TEC0 (0 km to LEO altitude) and the F3/C plasmaspheric content (LEO to GPS altitude).

This study applies the ground-based GNSS and F3/C TEC observations in March 2015 to construct the TGIMs every 5 min. The total numbers of F3/C and ground-based GNSS TEC observations are 20,797 (about 2 every 5 min.) and 7×10^7 (about 8000 every 5 min.), respectively, in this month. The number of the ground-based GNSS observation is much higher than that of the F3/C observation. However, the F3/C provides observation over areas such as oceans, desserts, and polar regions, where there rarely are ground-based GNSS receivers.

Construction of TIGER GIM

This section illustrates the construction of the high temporal resolution (5 min) TGIM in near-real time (4-h delay) by using the spherical harmonic expansion and Kalman filter update formula with TECs from ground-based GNSS receivers and the F3/C on the magnetic apex coordinates (Richmond 1995) using realistic geomagnetic fields (International Geomagnetic Reference Field, http://www.ngdc.noaa.gov/IAGA/vmod/ igrf.html). The flowchart shown in Fig. 2 shows that we first construct a global TEC map using the spherical harmonic expansion from ground-based GNSS TEC. The second step is to assimilate the 5-min F3/C TEC observation into the global TEC map using the Kalman filter update formula.

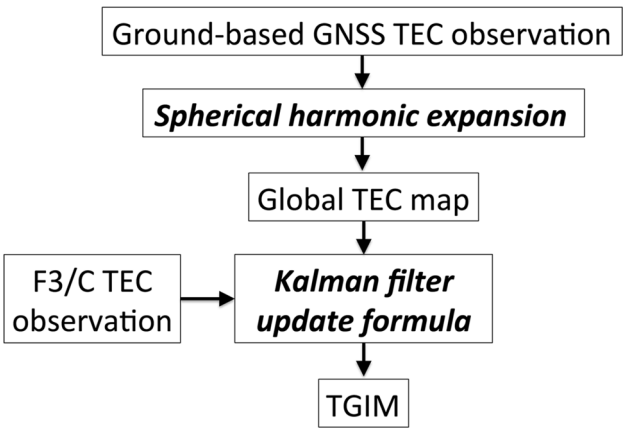

Fig. 2 Flowchart of the construction of the TIGER GIM (TGIM)

The equation describes the construction of a global TEC map using the spherical harmonic expansion (Schaer et al. 1996),

$$\mathrm{GIM}(\beta, s) = \sum_{n=0}^{n_{\max}} \sum_{m=0}^{n} \tilde{P}_{nm}(\sin\beta) \cdot (a_{nm} \cos ms + b_{nm} \sin ms) \quad (2)$$

where $\tilde{P}_{nm}$ is the normalized associated Legendre function of degree n (0,…,$n_{\max} = 15$) and order m (0,…,n); a_{nm} and b_{nm} are coefficients derived from least squares fitting of ground-based TEC observations; β is latitude; s is defined as t + longitude$-\pi$; and t is universal time (UT).

Figure 3 shows an example of construction of the TGIM at one time step. Panel (a) displays the TEC measured by the ground-based GNSS receivers from 1600 to 1605 UT on March 21, 2015. Since the TEC map constructed by using the ground-based TEC data and the spherical harmonic expansion may fluctuate a lot in regions where no ground-based GNSS receivers are located, Schaer et al. (1998) suggested that filling the data gap using pseudo-observations is greatly helpful for constraining the values. The pseudo-observation we used is the TGIM from previous time step by shifting 1.25° (360°/288) westward which is based on the assumptions that the global feature of TEC is sun synchronous and does not change a lot within a short period. Panel (b) is the TEC map constructed from ground-based GNSS TEC with the pseudo-observation using the spherical harmonic expansion.

The Kalman filter update formula (Welch and Bishop 1995) is an efficient way to assimilate both ground- and space-based observations into background model vectors, e.g., TEC from International Reference Ionosphere (IRI), and to construct a TEC map for monitoring the ionospheric weather (Fuller-Rowell et al. 2006; Lin et al. 2012; Sun et al. 2013). In this study, the global TEC map constructed by using the spherical harmonic expansion is treated as the background model vector. The Kalman filter update formula assimilates the F3/C TEC observations into the global TEC map and then the TGIM VTEC is given by

$$\mathrm{TGIM} = x + K(z - Hx) \quad (3)$$

in which

$$K = PH^T\left(HPH^T + R\right)^{-1} \quad (4)$$

where K is the Kalman gain; z and x represent the observation and background model vectors, which are obtained from the F3/C-observed TEC seen in panel (c) and the global TEC map, respectively. The background error covariance P is parameterized by a Gaussian function, $G(\beta, \alpha) = e^{-\frac{(\alpha-\alpha_R)^2+(\beta-\beta_R)^2}{2\alpha_w\beta_w}}$, where α and β are the longitude and latitude referring to the reference point at α_R and β_R. α_w

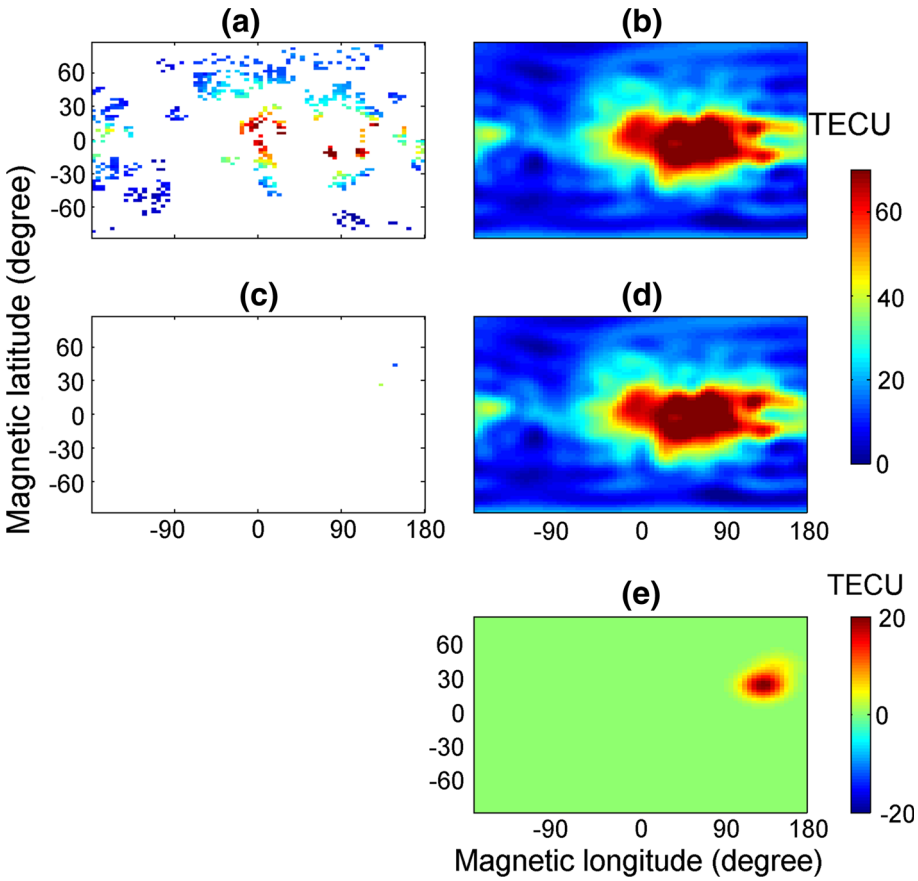

Fig. 3 Example of construction of the TGIM. **a** GNSS TEC observations, **b** global TEC map from the GNSS TEC observations, **c** two F3/C TEC observations, and **d** TGIM on geomagnetic coordinate at the time step of 1600–1605 UT on March 21, 2015. **e** The difference between the TGIM and the global TEC map displays the effect of the two F3/C data on the TEC values

and β_w are the widths of the bell-shaped surface of the Gaussian function in longitudinal and latitudinal directions, respectively. The measurement covariance R is a diagonal matrix. Values of R are assumed to be ten times smaller than P. As R approaches zero, the measurement is trusted much more than the background vector. The H operator is an identity matrix since both the background and observational vectors have the same unit. We assume these covariance matrices are constant throughout the entire procedure. Panel (e) is the difference between the TGIM seen in panel (d) and the global TEC map seen in panel (b) at the time step of 1600–1605 UT. It displays the enhancement caused by the F3/C TEC near 30°N, 140°E.

The Kalman filter update formula with the covariance matrices has been applied to construct the regional TEC map over the continent of USA to study the storm-enhanced density (Sun et al. 2013) and to assimilate F3/C electron density peak height into the ionosphere plasmasphere model to get the better thermospheric neutral wind and electron density (Sun et al. 2015). The covariance matrixes computing from data or background vectors will be considered if the prediction part is included. Sun et al. (2013) estimated the nonstationary wavelet-based background model error covariance from the ground-based GNSS TEC observations. Lin et al. (2015) derived the nonstationary background model error covariance from the IRI-simulated electron density profiles.

Figure 4 shows the impact of the F3/C TEC data on the TEC map using the spherical harmonic expansion. The top panel is the TEC map constructed from the ground-based GNSS and the two F3/C TEC observations using the spherical harmonic expansion at the step of 1600–1605 UT. The bottom panel shows the differences between the TEC maps with and without including the two F3/C TEC data. The difference pattern is similar to that of Fig. 3e, but the values are smaller. The reason for the weaker influence is because the fitting using the global spherical harmonics tends to smooth out the local influence from the data. The Kalman filter update formula with the covariance is designed for spreading the influence of the data on the background model vectors locally.

Results

Figure 5 shows a snapshot of the TGIM at the time step of 1600–1605 UT on March 21, 2015, compared with the GIMs published by CODE, ESOC, UWM, JPL, and UPC at 1600 UT. All these GIMs show the typical latitudinal and longitudinal variations in TEC at the one time step. Figure 6

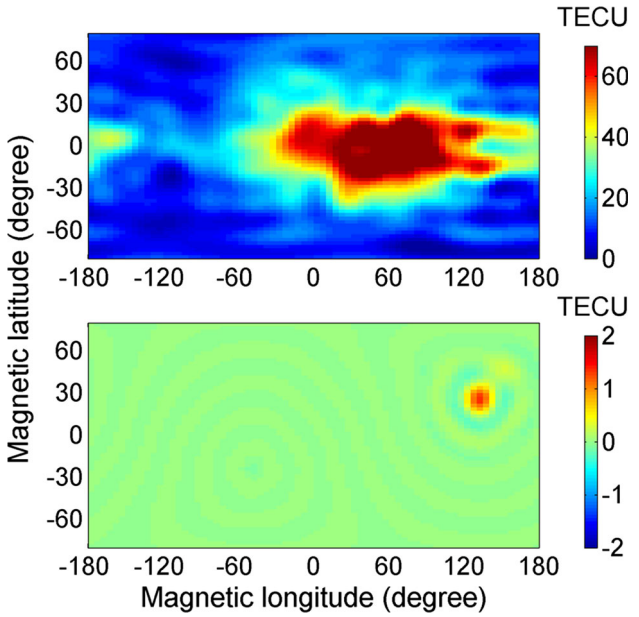

Fig. 4 Effect of the F3/C TEC on the global TEC map using the spherical harmonic expansion. (*Top*) TEC map constructed from the ground-based GNSS and the two F3/C TEC observations at the time step of 1600–1605 UT on March 21, 2015. (*Bottom*) Differences between the TEC maps with and without including the two F3/C TEC observations

displays the correlations between the TGIM and the entire data set of the other GIMs collected in March 2015. The high correlation (correlation coefficients are near 0.95) reveals that the overall features of those GIMs are similar.

To show how much the TGIM differs from the GIMs of other centers, the root mean square (RMS) between the TGIM and the rest of the GIMs has been estimated and is shown in Fig. 7. The monthly averaged global RMS values between TGIM and CORG, EHRG, IGRG, JPRG, and UHRG are 7.68, 7.00, 7.52, 9.05, and 7.95 TECU, respectively. The 7–9 TECU differences can be attributed to the following reasons: (1) The construction of the TGIM is based on the data collected within a 5-min time interval that is much short than the other GIMs. (2) The TGIM is constructed on the apex coordinates that differs from the other GIMs.

The time series of RMS estimated at each latitude belt show the differences in detail. As shown in Fig. 7, the TGIM is closer to the other GIMs in the Northern Hemisphere. The smaller difference is a result of most ground-based GNSS receivers being located in the Northern Hemisphere. The larger discrepancy in the Southern Hemisphere can be attributed to different satellite data sets being involved in the different GIM systems.

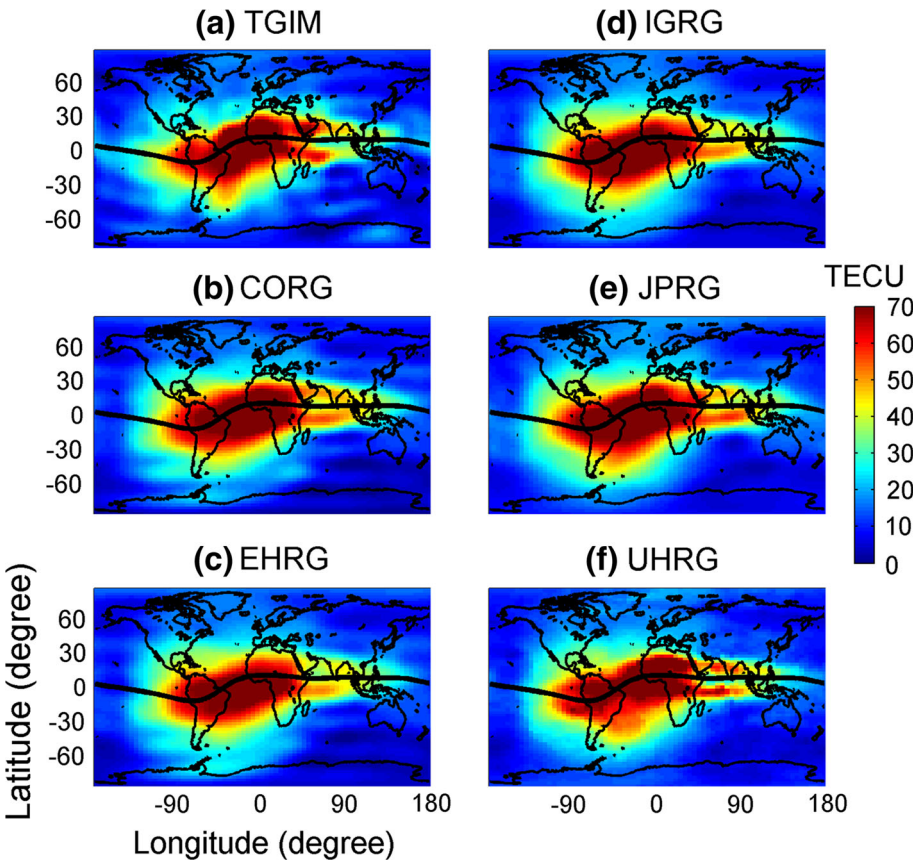

Fig. 5 Snapshots of global TEC structures in the GIMs at 1600 UT on March 21, 2015. **a** TGIM and the GIMs published by **b** CODE (CORG), **c** ESOC (EHRG), **d** UWM (IGRG), **e** JPL (JPRG), and **f** UPC (UHRG)

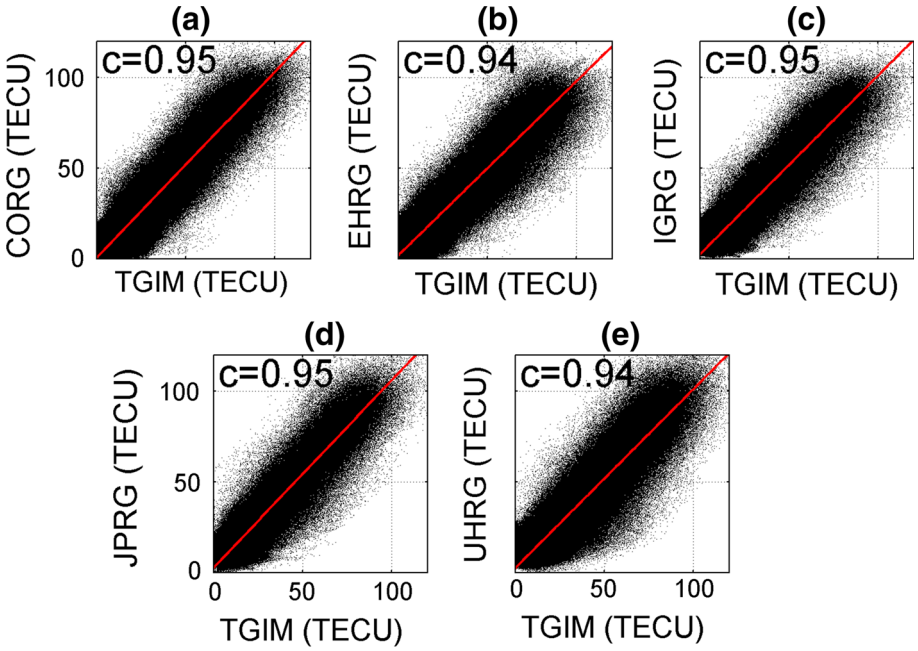

Fig. 6 Correlation between the TGIM and the other GIMs published by **a** CODE, **b** ESOC, **c** UWM, **d** JPL, and **e** UPC in March 2015. The entire data sets of the GIMs in this month are used to compute the correlations. *Red line* is the linear regression line

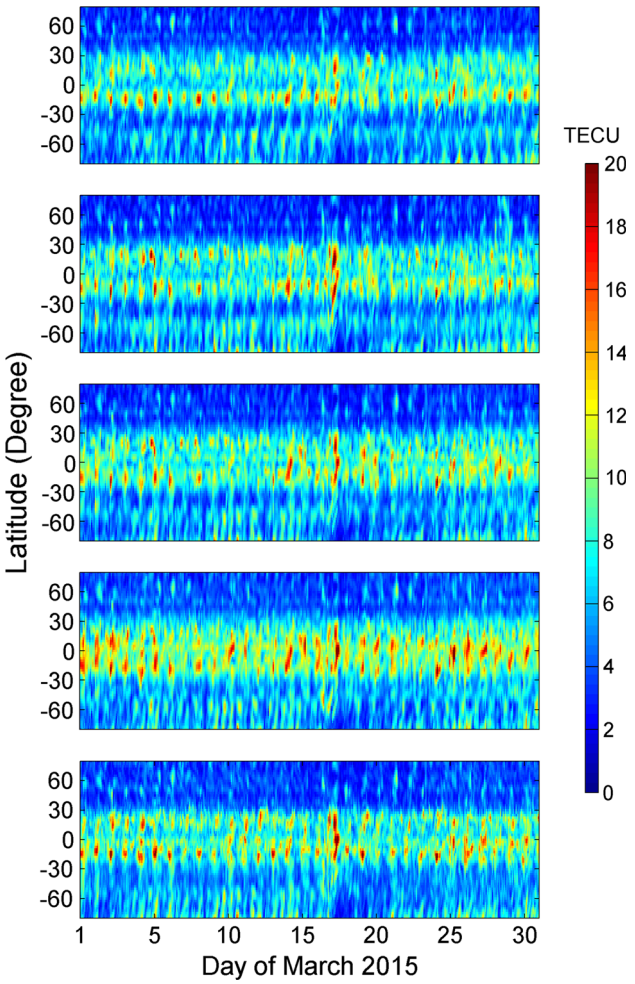

Fig. 7 Time series of root mean square between TGIM and CORG, EHRG, IGRG, JPRG, and UHRG (from *top* to *bottom*) in March 2015

The F3/C soundings are distributed nearly uniformly around the globe. Such coverage provides an excellent opportunity to fill the data gap of the ground-based GNSS TEC observations over the ocean, dessert, and polar areas. To show the impact of the F3/C TEC on the GIM, the global TEC map constructed only using ground-based GNSS TEC and the TGIM is validated with the TECs observed by Ocean Surface Topography Mission (OSTM)/Jason-2. The altimeters on board OSTM/Jason-2 satellites observe the nadir vertical TEC over the ocean region (Dumont et al. 2009). Figure 8 shows the global distribution of the RMS between the OSTM/Jason-2 and GIM TECs in March 2015. In this validation, we first take the difference between the TGIM and the OSTM/Jason-2 TECs along the satellite ground track every 5 min per day, and then, the RMS is computed from the differences accumulated at each grid point over the entire month. The F3/C TEC exhibits improvement on the GIM over the ocean areas of about 15.5% ((8.31 TECU–7.02 TECU)/8.31 TECU). It also shows that assimilating of the F3/C TEC improved the TEC map at middle and high latitudes of the Southern Hemisphere, especially the areas without ground-based GNSS receivers.

Discussion and conclusion

The high correlation between the TGIM and the GIMs made available by the other five international organizations suggests that the 5-min resolution TGIM is reliable to show the overall features of global TEC. The near-real-time TGIM allows scientists to not only evaluate the quality of communication, positioning, and navigation applications, but also study the ionospheric plasma physics and explore

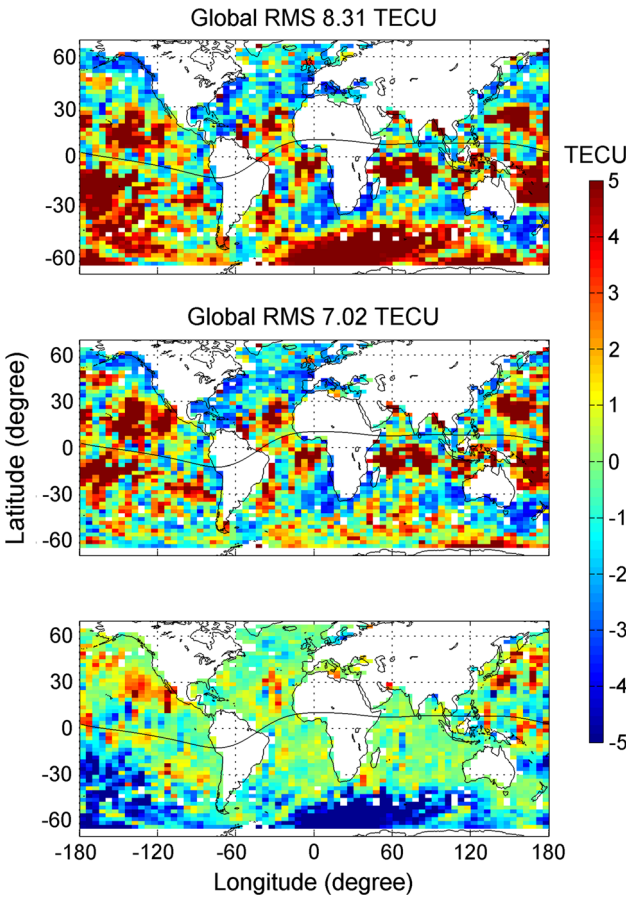

Fig. 8 Impact of the F3/C TEC on the GIM over the ocean area in March 2015. Global distributions of the RMS of the differences between the OSTM/Jason-2 TEC and the GIM without (*top*) and with (*middle*) the F3/C TEC, respectively, as computed from the TEC differences at each grid point. *Bottom*: Difference between RMS values shown in *top* and *middle* panels. *Blue* indicates the reduction in the RMS if the F3/C TEC was assimilated

new sciences and findings, as well as assess the hazard of forthcoming large earthquakes (Liu et al. 2009, 2010, 2011).

Following the success of F3/C, an additional 12 small satellites of FORMOSAT-7/COSMIC-2 (F7/C2) will be launched in 2018 and 2019. The upcoming F7/C2 satellite mission will provide at least four times the amount of data of F3/C, which results in a dense coverage. This new satellite constellation mission is twice as larger than the former and will provide 8000–10,000 space-to-space Global Navigation Satellite System (GNSS) observations per day. We expect that the denser RO soundings for F7/C2 can yield more improvement on the GIM.

The near-real-time TGIM can be used to quickly provide horizontal structure of ionospheric electron density to the data assimilation procedure (Lin et al. 2015). This procedure can produce three-dimensional (3D) ionospheric electron density structure for monitoring of space weather in near-real time. That benefits comprehensive studies of ionospheric quiet/storm time condition, ionosphere–thermosphere interaction, and physical characteristic of ionosphere such as sudden stratosphere warming, Weddell Sea anomaly, electrodynamics, $\boldsymbol{E} \times \boldsymbol{B}$ drift, as well as ionospheric earthquake precursor studies. Moreover, the 3D covariance matrices estimated from observations or simulations can be further updated if the Kalman filter time update formula is included for the prediction purpose (Welch and Bishop 1995).

In conclusion, F3/C ionospheric RO soundings significantly improve the TGIM over the ocean areas, especially in the Southern Hemisphere. The near-real-time TIGER GIM highly correlates with the GIMs released by the other five international organizations, which allows scientists to study the ionospheric weather related to magnetic storms, sudden stratospheric warming, midlatitude trough, midlatitude summer night anomaly, and the seismo-ionospheric precursors.

Acknowledgments This study is supported by the grant of Ministry of Science and Technology to National Central University, MOST 104-2628-M-008-001, to National Cheng Kung University, MOST 105-2111-M-006-004, and the ISSI-Bern International Team of "Ionospheric Space Weather Studied by RO and Ground-based GNSS TEC Observations" (the team leader Liu J. Y. (TW)). The authors gratefully acknowledge Taiwan Analysis Center for COSMIC (TACC) for providing the near-real-time GNSS TEC data, as well as CDAAC and TACC for publishing F3/C RO data, and NASA/JPL for providing the OSTM/Jason-2 data (ftp://podaac-ftp.jpl.nasa.gov/allData/ostm/). The authors would like to thank the reviewers for their comments that help improve the paper.

References

Davies K (1990) Ionospheric radio. IEEE Electromagnetic Waves Series 31

Dumont JP, Rosmorduc V, Picot N, Desai S, Bonekamp H, Figa J, Lillibridge J, Scharroo R (2009) OSTM/Jason-2 products handbook. Jet Propul Lab, Pasadena

Fuller-Rowell TJ, Araujo-Pradere EA, Minter C, Codrescu M, Spencer P, Robertson D, Jacobson AR (2006) US-TEC: a new data assimilation product from the space environment center characterizing the ionospheric total electron content using real-time GPS data. Radio Sci 41:RS6003. doi:10.1029/2005RS003393

Hernández-Pajares M, Juan JM, Sanz J, Orus R, Garcia-Rigo A, Feltens J, Komjathy A, Schaer SC, Krankowski A (2009) The IGS VTEC maps: a reliable source of ionospheric information since 1998. J Geod 83(3):263–275. doi:10.1007/s00190-008-0266-1

Huang CM, Chen MQ, Liu JY (2010) Ionospheric positive storm phases at the magnetic equator close to sunset. J Geophys Res 115:A07315. doi:10.1029/2009JA014936

Jin R, Jin S, Feng G (2012) M_DCB: matlab code for estimating GNSS satellite and receiver differential code biases. GPS Solut 16(4):541–548. doi:10.1007/s10291-012-2790-3

Jin S, Jin R, Hutoglu H (2017) Positive and negative ionospheric responses to the March 2015 geomagnetic storm from BDS observations. J Geod. doi:10.1007/s00190-016-0988-4

Lin CY, Liu JY, Lin CH, Sun YY, Araujo-pradere EA, Kakinami Y (2012) Using the IRI, the MAGIC model, and the co-located ground-based GPS receivers to study ionospheric solar eclipse

and storm signatures on July 22, 2009. Earth Planets Space 64:513–520. doi:10.5047/eps.2011.08.016

Lin CY, Matsuo T, Liu JY, Lin CH, Tsai HF, Araujo-Pradere EA (2015) Ionospheric assimilation of radio occultation and ground-based GPS data using non-stationary background model error covariance. Atmos Meas Tech 8:171–182. doi:10.5194/amt-8-171-2015

Liu JY, Chen YI, Chen CH, Liu CY, Chen CY, Nishihashi M, Li JZ, Xia YQ, Oyama KI, Hattori K, Lin CH (2009) Seismoionospheric GPS total electron content anomalies observed before the 12 May 2008 Mw7.9 Wenchuan earthquake. J Geophys Res 114:A04320. doi:10.1029/2008JA013698

Liu JY, Chen YI, Chen CH, Hattori K (2010) Temporal and spatial precursors in the ionospheric global positioning system (GPS) total electron content observed before the 26 December 2004 M9.3 Sumatra–Andaman Earthquake. J Geophys Res 115:A09312. doi:10.1029/2010JA015313

Liu JY, Le H, Chen YI, Chen CH, Liu L, Wan W, Su YZ, Sun YY, Lin CH, Chen MQ (2011) Observations and simulations of seismoionospheric GPS total electron content anomalies before the 12 January 2010 M7 Haiti earthquake. J Geophys Res 116:A04302. doi:10.1029/2010JA015704

Richmond AD (1995) Ionospheric electrodynamics using magnetic apex coordinates. J Geomag Geoelectr 47:191–212. doi:10.5636/jgg.47.191

Schaer S, Beutler G, Mervart L, Rothacher M, Wild U (1995) Global and regional ionosphere models using the GPS double difference phase observable. In: Proceedings of the IGS workshop on special topics and new directions, Potsdam, Germany, May 15–17, 77–92

Schaer S, Beutler G, Rothacher M (1996) Daily global ionosphere maps based on GPS carrier phase data routinely produced by the CODE analysis center. In: Proceedings of the IGS analysis center workshop, Silver Spring, MD, USA, 181–192

Schaer S, Beutler G, Rothacher M (1998) Mapping and predicting the ionosphere. In: Proceedings of the IGS analysis center workshop, Darmstadt, Germany, February 9–11, 307–318

Sun YY, Matsuo T, Araujo-Pradere EA, Liu JY (2013) Ground-based GPS observation of SED-associated irregularities over CONUS. J Geophys Res Space Phys 118:2478–2489. doi:10.1029/2012JA018103

Sun YY, Matsuo T, Maruyama N, Liu JY (2015) Field-aligned neutral wind bias correction scheme for global ionospheric modeling at midlatitudes by assimilating FORMOSAT-3/COSMIC $h_m F_2$data under geomagnetically quiet conditions. J Geophys Res Space Phys 120:3130–3149. doi:10.1002/2014JA020768

Tsai HF, Liu JY (1999) Ionospheric total electron content response to solar eclipses. J Geophys Res 104(A6):12657–12668. doi:10.1029/1999JA900001

Welch G, Bishop G (1995) An introduction to the Kalman filter. Technical Report 95-041, Department of Computer Science, University of North Carolina at Chapel Hill

Zhang X, Tang L (2014) Daily global plasmaspheric maps derived from cosmic GPS observations. IEEE Trans Geosci Remote Sens 52(10):6040–6046

Yang-Yi Sun is a postdoctoral researcher at National Central University (NCU), Taiwan, since he obtained Ph.D. degree at NCU in 2014. His research interests include space weather and thermosphere–ionosphere coupling. He worked on analyzing and assimilating ground- and space-based GNSS data for studying these scientific topics for several years.

Jann-Yenq Liu received a BS from the Atmospheric Physics Department, National Central University (NCU), Taiwan, in 1980, and a Ph.D. from the Physics Department, Utah State University, USA, in 1990. He is a professor at Institute of Space Science, NCU. His research areas are in ionospheric space weather, ionospheric data assimilation, seismo-traveling ionospheric disturbances, and ionospheric earthquake precursors by GPS radio occultation and ground-based GNSS observations.

Ho-Fang Tsai received his Ph.D. degree in Space Science in 1999 at National Central University in Taiwan. His scientific interests include ground- and space-based GNSS application on ionospheric/plasmaspheric morphology and disturbances related to earthquakes and tsunamis. Currently he is an associate researcher at National Cheng Kung University and focuses on GNSS radio occultation ionospheric development for FORMOSAT-7/COSMIC-2 mission.

Andrzej Krankowski has an extensive research experience in developing algorithms for precision monitoring of the ionosphere. Currently, his algorithms provide high spatial and temporal resolution of TEC maps and represent all local and regional features of the TEC distribution (associated with geomagnetic storms, solar flares, solar eclipses, and seismic events). Recently he became Chairman of the IGS Ionosphere Working Group.